View metadata, citation and similar papers at core.ac.uk
brought to you by CORE
provided by Digital Repository @ Iowa State University

APPLICATIONS OF DIGITAL IMAGE ENHANCEMENT TECHNIQUES FOR IMPROVED ULTRASONIC IMAGING OF DEFECTS IN COMPOSITE MATERIALS

Brian G. Frock and Richard W. Martin

University of Dayton
Research Institute
Dayton, Ohio 45469

ABSTRACT

Several standard digital image enhancement techniques have been applied to digitized ultrasonic C-scan images of defects in graphite/epoxy composites. Features in the computer enhanced images are much more distinct than those in the original images. In some cases, cracks which are too close together to be visually resolved in the original images are clearly resolved in the enhanced images. Noisy images have been improved by first smoothing the original data and then edge enhancing the smoothed data. The resulting sharpened edges improve the visualization of features in the images. The application of digital image enhancement techniques has allowed the imaging of defects in composite materials at frequencies as low as 3.5 MHz. This use of these lower frequencies permits better imaging of defects in thick composite materials.

INTRODUCTION

Ultrasonic C-scan images which have not been created from digitized and stored data often fail to display all of the information which is available. This is due primarily to the necessity of setting the breakpoints between grey levels prior to scanning rather than after the scan has been completed. Digitizing and storing the data overcomes these problems because the number of grey levels and their threshold values are selected after the scanning is completed. This allows the image to be displayed as often as desired and with an almost unlimited number of different choices of threshold values. More importantly, digital image enhancement techniques which have been developed and used in other disciplines [1-3] can now be applied in the field of ultrasonic NDE.

In this paper we demonstrate how some of the more common digital image enhancement techniques can be applied to the ultrasonic NDE of graphite/epoxy composites to improve the visualization and spatial resolution of image features of interest.

SCANNING AND DISPLAY SYSTEMS

A high-precision, computer controlled scanning system was developed for the acquisition, storage, enhancement, and display of ultrasonic images of up to 512 x 512 points in size. Control of the system is accomplished by an LSI-11/23 microcomputer with an RT-11 operating system through a high speed IEEE-488 DMA interface to a data acquisition module and a stepper motor controller. A schematic diagram of the system and additional information are available in prior publications [4-5].

The video display system is capable of displaying from 2 to 16 colors or levels of grey-scale representing the signal amplitude. The user has the option of selecting equal percent of range thresholding, equalized histogram thresholding, or the user may specify the threshold values. The number of breakpoints can also be selected by the user.

DIGITAL IMAGE ENHANCEMENT TECHNIQUES

With the exception of histogram equalization and edge sharpening by blurred image subtraction, the image enhancement techniques presented in this paper were implemented through the use of a moving 3 pixel by 3 pixel mask. The numbering system for the individual elements in the mask is illustrated in Fig. 1a.

Mean Value Filter

The simplest of the techniques is the mean value filter [6] in which the amplitude of the central pixel in the mask is replaced by the mean value of the amplitudes of the nine pixel elements within the mask. This type of filter is used mostly for noise removal in cases where the noise severely interferes with visual interpretation of image features, and for preprocessing to remove low level noise in images which will be subjected to high frequency enhancements for improved edge detection and visualization.

Edge Enhancement by First Differences

There are a large number of directional edge enhancement techniques described in the literature [2,3,7-11]. Most of the techniques use an approximation to the first derivative in which the amplitude of the central pixel in the original image is replaced by the sum of first differences of pixel amplitudes within the mask. The first difference mask [3] which we used for vertical edge enhancements is given in Fig. 1b. If the difference in pixel amplitudes across the vertical region enclosed by the mask is large and positive, the value of the corresponding central pixel in the transformed image will be large and positive. If the difference is large and negative, the value of the corresponding central pixel in the transformed image will be large and negative. Not only are vertical edges enhanced, but they are also directionally "shaded", thus creating a three-dimensional effect. The mask [3] used in this paper for horizontal edge enhancement is given in Fig. 1c. Horizontal edges in the resultant image are both sharpened and shaded.

Images which are both visually pleasing and very useful for feature identification can be created by adding the vertical edge enhanced image to the horizontal edge enhanced image. The resultant image has sharpened edges and directionally dependent shading which creates a three-dimensional effect. The mask for this transformation is given in Fig. 1d.

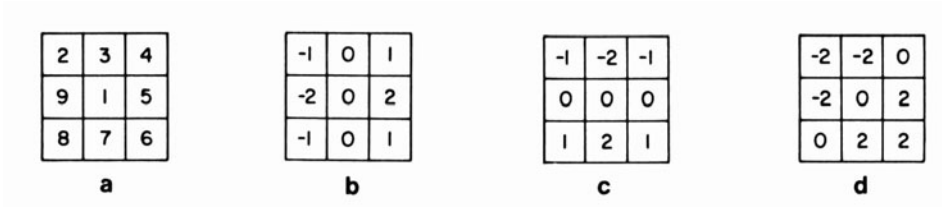

Fig. 1. Enhancement masks: (a) Numbering system; (b) First difference vertical edge enhancement; (c) First difference horizontal edge enhancement; (d) Sum of "b" and "c".

Edge Enhancement by Blurred Image Subtraction

Castleman [1] has demonstrated that when the blurred image is subtracted from the original image, the higher spatial-frequency image which results has sharpened edges with bands on both sides of the edges. As Hall, et al. [11] point out, this banding aids the visual detection of the edges and improves feature identification. No directional shading is produced by this technique, and thus the image has no three-dimensional appearance.

Histogram Equalization

Histogram equalization [2] sets the grey level thresholds for image display such that each grey level has approximately the same number of pixel elements. Thus, most of the grey level thresholds are placed in the regions of the image histogram where most of the pixel amplitudes occur. This greatly increases the probability that amplitudes of pixels on different sides of an edge will be placed in different grey levels, and increases the probability that the edge will be visible.

SAMPLE

The sample used for this study is a 16 ply graphite/epoxy specimen with a $[90_4/0_4]_s$ fiber orientation. Its physical dimensions are 6.4 cm long by 2.5 cm wide by 0.25 cm thick. The sample contains matrix cracks in both of the 90 degree plies and also in the 0 degree plies (see Fig. 2).

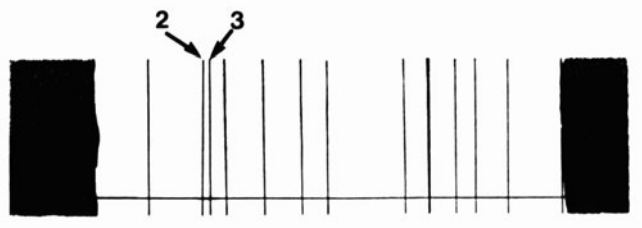

Fig. 2. X-ray radiograph of cure crack sample.

DATA COLLECTION

The data were collected using normal incidence ultrasonic immersion C-scanning techniques with focused transducers. Three different transducers with the following parameters were used: (1) 25 MHz center frequency, 0.64

cm diameter, 2.54 cm focal length; (2) 10 MHz center frequency, 1.27 cm diameter, 7.6 cm focal length; and (3) 3.5 MHz center frequency, 1.27 cm diameter, 5.1 cm focal length. For each transducer data were acquired with the transducer focused on the front surface of the sample and also with the transducer focused on the back surface of the sample (not all of the data are presented here).

In all cases the RF echoes were pre-amplified, then further amplified, rectified and low-pass filtered (5 MHz cutoff) with a MATEC Broadband Receiver. An electronic gate was centered over the rectified and filtered back surface echo and the averaged value of the gated signal was digitized and stored during scanning. The step sizes for all scans were 0.013 cm by 0.013 cm.

Near noiseless images were generated by using small amounts of attenuation in the pre-amplifier stage and little gain in the Broadband Receiver stage. A noisy image was generated by using more attenuation in the pre-amplifier stage. The signal which was subsequently amplified at the Broadband Receiver stage had a much lower signal-to-noise ratio and produced a noisy image.

IMAGES

Typical binary C-scan images are presented in Figs. 3a and 3b. Data for these images were collected with the 25 MHz transducer focused on the front surface of the sample. Since the amplitude of the back surface echo was used to produce the image, discontinuities appear as white areas on a black background. Some of the cracks are readily visible in Fig. 3a where the threshold was set at 50% of the range. When the threshold level was raised to 70% of the range (Fig. 3b), more of the cracks became visible, but other features also appeared.

Better visual images of the sample are shown in Figs. 3c and 3d. All sixteen grey levels are used for these images rather than just two as was the case for Figs. 3a and 3b. The image in Fig. 3c is displayed using an equal percent of range thresholding, whereas the image in Fig. 3d is displayed in an equalized histogram threshold format. Clearly, more visual information is made available to the viewer through the use of the equalized histogram display format. The very narrow vertical and horizontal lines which are visible in Fig. 3d are the result of surface irregularities caused by the bleeder cloth during the fabrication process.

Comparison of the images in Fig. 3 with the X-ray radiograph in Fig. 2 reveals that not all of the cracks in the sample have been imaged by the ultrasonic interrogation. This is due to the very short acoustic depth of field of the transducer used for the data collection. Those cracks in the upper 90 degree plies are sharply imaged, while those in the lower 90 degree plies are out of focus and are too blurred to be visually identified.

An enhanced version of the images of Fig. 3 is shown in Fig. 4. This image was created by first smoothing the data with a mean value filter and then subtracting the mean value filtered (blurred) version from the original image. Several characteristics are evidenced in this image. First, the cracks are more precisely defined than in the previous images. Second, the low spatial-frequency variations in image intensity have been removed, producing an image which is much more uniform in intensity than the previous images. Third, the surface texture is visible over the entire image. Finally, there are some dark bands on both sides of most of the cracks which aid the eye in the detection of the cracks.

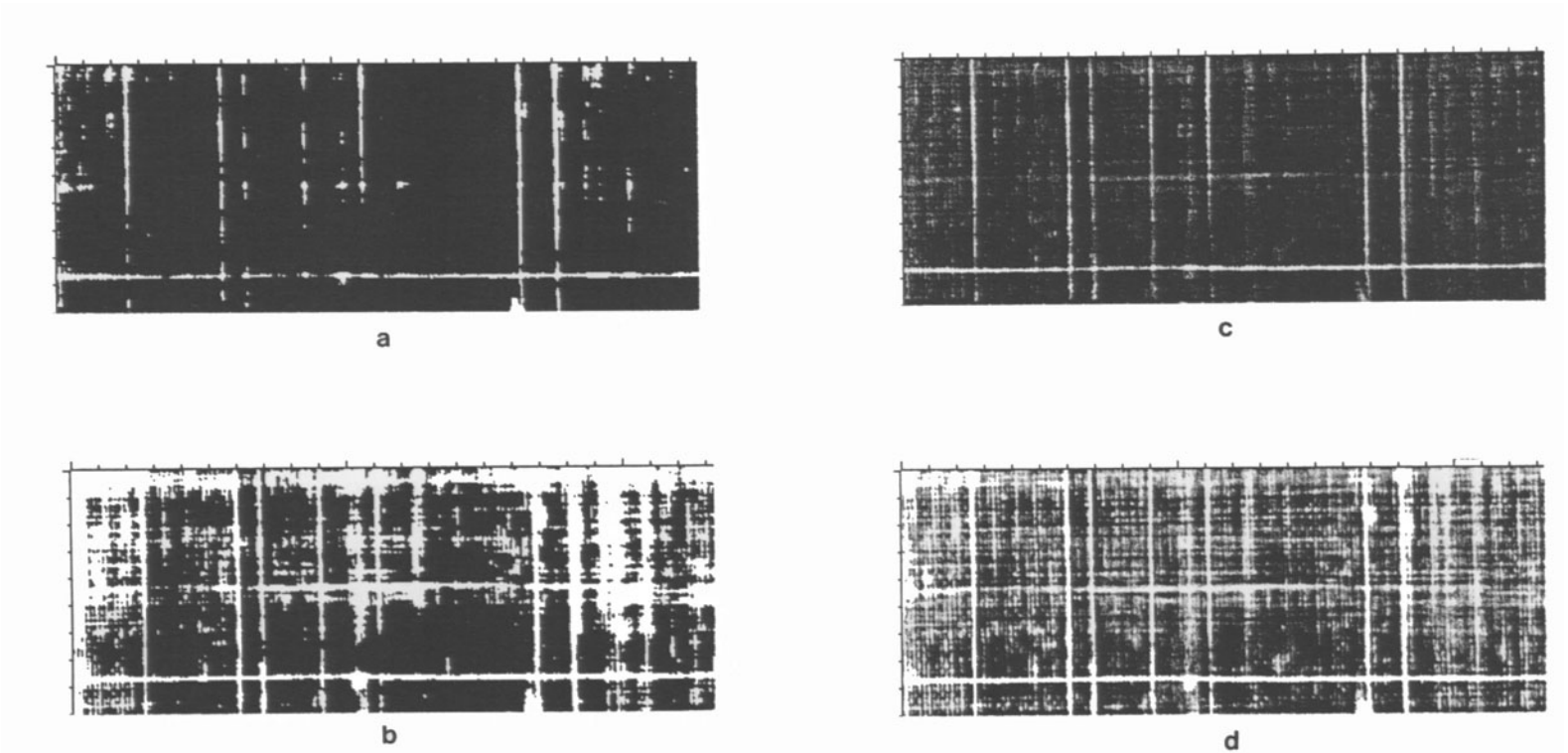

Fig. 3. Images of cure crack sample using 25 MHz transducer: (a) Binary image with threshold at 50% of range; (b) Binary image with threshold at 70% of range; (c) Sixteen grey-level image, equal percent of range thresholding; (d) Sixteen grey-level image, equalized histogram thresholding.

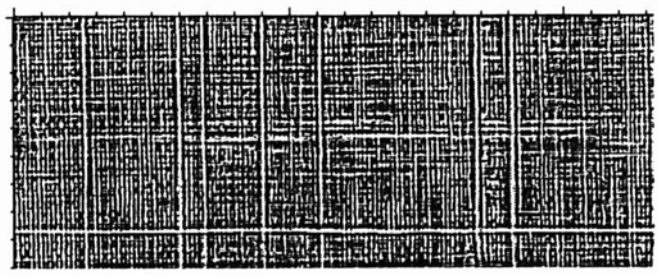

Fig. 4. Edge enchanced version of images in Fig. 3 using blurred image subtraction technique.

Images generated from data acquired with the 10 MHz transducer focused on the back surface of the sample are presented in Fig. 5. Cracks in all of the plies are visible because of the longer acoustic depth of field of this transducer. The unenhanced data is displayed in a 16 grey level equalized histogram format in Fig. 5a. Note in particular the cracks labeled 2 and 3 in Fig. 5a and in the X-ray radiograph of Fig. 2. Crack number 2 is in the bottom 90 degree ply layer while crack number 3 is in the top 90 degree ply layer. An edge enhanced version of the image in Fig. 5a is presented in Fig. 5b. This image was generated by summing the vertically and horizontally edge enhanced version of the data which was used to generate the image in Fig. 5a. The image in Fig. 5b has a pseudo three-dimensional appearance which produces the illusion that the cracks are elevated above the background. The two cracks (labeled 2 and 3) are also more visible in this image than in the original image.

A noisy 10 MHz image of the sample is shown in Fig. 5c. In this image the cracks labeled 2 and 3 are blurred together and are not clearly discernable. Fig. 5d shows the same data after three consecutive passes with a mean value filter followed by horizontal and vertical edge enhancements. This image is the sum of the vertically and horizontally edge enhanced versions of the smoothed image. The pseudo three-dimensional appearance is present, and cracks 2 and 3 are visually resolvable.

Images generated by using the 3.5 MHz transducer to insonify the sample are presented in Fig. 6. Data for Fig. 6a were acquired with the transducer focused on the front surface of the sample, while the data for Fig. 6b were acquired with the transducer focused on the back surface of the sample. Outlines of the cracks are fuzzy, and cracks 2 and 3 are not resolvable. There is, however, some evidence in Fig. 6c that the two cracks are resolvable when the images of Fig. 6a and 6b are suitably combined. Generation of this image from the two previous images required multi-stage processing techniques. First the data for Fig. 6b was subtracted from the data of Fig. 6a. Then, vertically and horizontally edge enhanced versions of the subtraction image were generated. Finally, the vertically and horizontally edge enhanced images were added together to create the image in Fig. 6c. The cracks are more distinct in this image, and cracks 2 and 3 are visually resolvable.

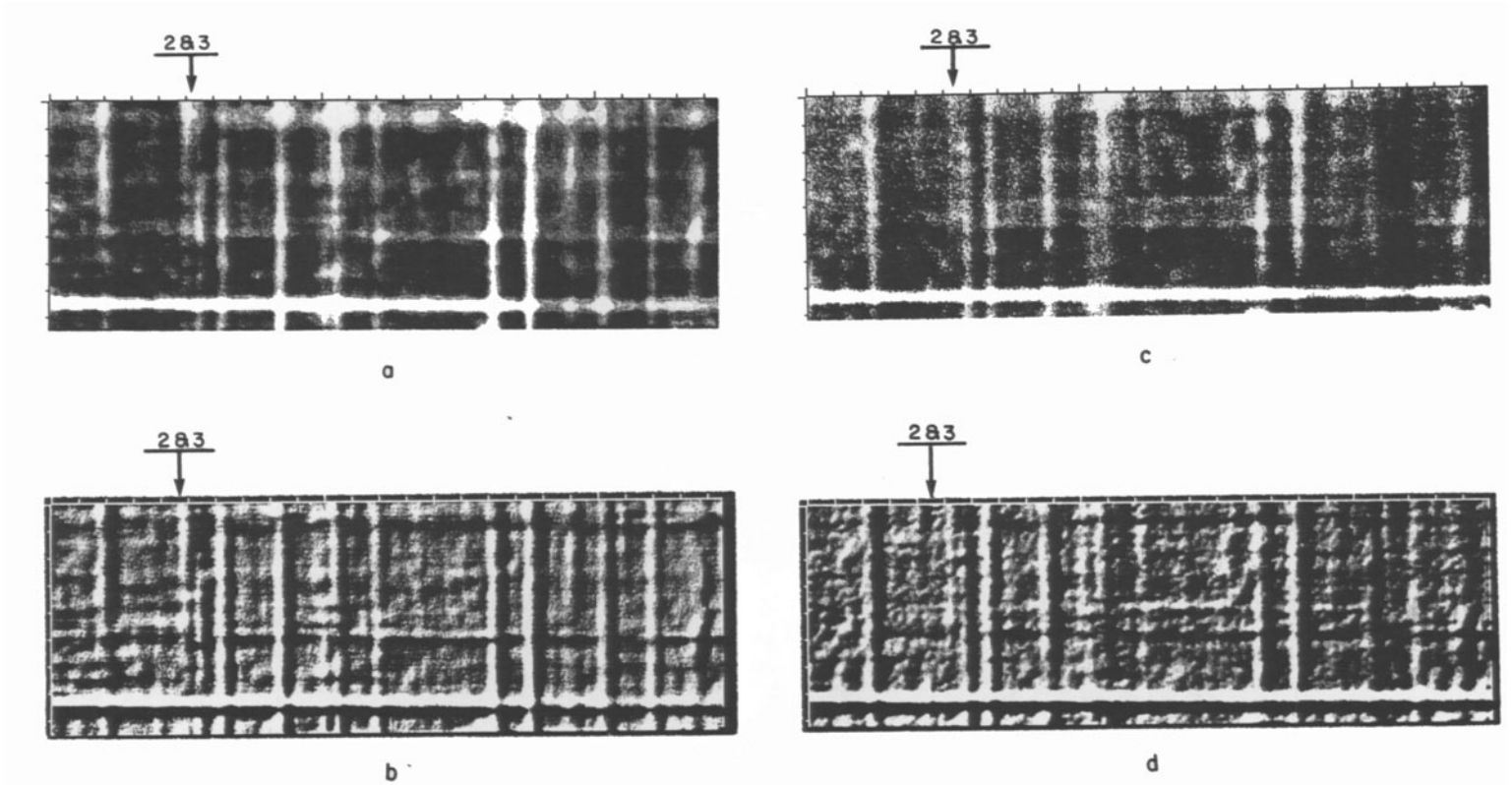

Fig. 5. Images of cure crack sample using 10 MHz transducer: (a) Low noise image; (b) Sum of first difference vertical and horizontal edge enhanced versions of "a"; (c) Noisy image; (d) Sum of first difference vertical and horizontal edge enhanced versions of "c" after mean value filtering.

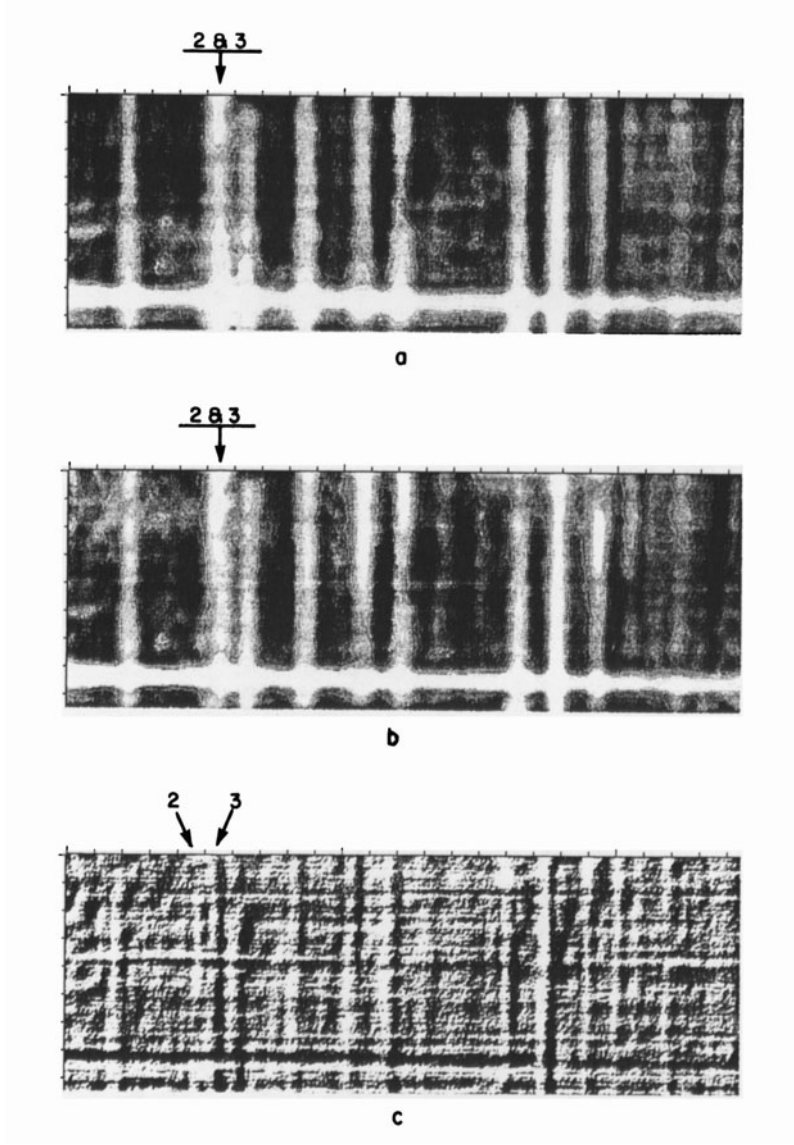

Fig. 6. Images of cure crack sample using 3.5 MHz transducer: (a) Transducer focused on front surface; (b) Transducer focused on back surface; (c) Sum of first difference vertical and horizontal edge enhanced versions of subtraction image ("a" minus "b").

SUMMARY

We have demonstrated how some very simple digital image processing techniques can be used to significantly improve the visibility of features in images generated from ultrasonic data. Further, we have demonstrated how some of these techniques can be applied to significantly improve the spatial resolution of features in images generated from data acquired at frequencies as low as 3.5 MHz. This is very important for the inspection of graphite/epoxy composite because of the large amounts of ultrasonic energy scattering which occur at temporal frequencies above 5 MHz.

ACKNOWLEDGMENTS

This research was sponsored by the AFWAL Materials Laboratory under Contract Number F33615-83-C-5036. The authors acknowledge Dr. Thomas J. Moran and Mr. Robert J. Andrews for their support and encouragement in the area of image enhancements. The authors also thank Mr. Mark Ruddell for his data collection efforts.

REFERENCES

1. K. R. Castleman, "Digital Image Processing," Prentice-Hall Inc., Englewood Cliffs, New Jersey, (1979).
2. R. C. Gonzalez and P. Wintz, "Digital Image Processing," Addison-Wesley Publishing Company, Reading Massachusetts, (1977).
3. H. C. Andrews and B.R. Hunt, "Digital Image Restoration," Prentice-Hall Inc., Englewood Cliffs, New Jersey, (1977).
4. T. J. Moran, R. L. Crane and R. J. Andrews, High Resolution Imaging of Microcracks in Composites, Materials Evaluation, Vol. 43, No. 5, (April 1985), pp 536-540.
5. R. W. Martin and R. J. Andrews, Backscatter B-Scan Images of Defects in Composites in: "Review of Progress in Quantitative Nondestructive Evaluation," Vol. 5, Plenum Press, (1986), pp 1189-1198.
6. J. Lee, Digital Image Enhancement and Noise Filtering by Use of Local Statistics, IEEE Transactions on Pattern Analysis and Machine Intelligence, Vol. PAMI-2, No. 2, (1980), pp 165-168.
7. L. S. Davis, A Survey of Edge Detection Techniques, Computer Graphics and Image Processing, 4, (1975), pp 248-270.
8. W. Frei and C. Chen, Fast Boundary Detection: A Generalization and a New Algorithm, IEEE Transactions on Computers, Vol. C-26, No. 10, (1977), pp 988-998.
9. A. Rosenfeld and M. Thurston, Edge and Curve Detection for Visual Scene Analysis, IEEE Transactions on Computers, (May 1971), pp 183-190.
10. J. E. Hall and J. D. Awtrey, Real-Time Image Enhancement Using 3 x 3 Pixel Neighborhood Operator Functions, Optical Engineering, Vol. 19, No. 3, (1980), pp 421-424.
11. E. L. Hall, R. P. Kruger, S. J. Dwyer, D. L. Hall, R. W. McLaren and G. S. Lodwick, A Survey of Preprocessing and Feature Extraction Techniques for Radiographic Images, IEEE Transactions on Computers, Vol. C-20, No. 9, (1971), pp 1032-1044.